12th IEA Heat Pump Conference 2017

Dynamic Modeling of a Personal Cooling Device with PCM Storage

Rohit Dhumane[a], Jiazhen Ling[a], Vikrant Aute[a], Reinhard Radermacher[a]

[a]Center for Environmental Energy Engineering, University of Maryland, College Park, 4164 Glenn Martin Hall, MD 20742, USA

Abstract

A personal cooling device, named Roving Comfort (RoCo), has been designed and a prototype has been fabricated at the Center for Environmental Energy Engineering. RoCo is capable of following occupant(s) autonomously and providing cooling/heating as needed. The device helps reducing building electricity consumptions by enabling extended thermostat settings for building air conditioning systems, i.e., 4°F above or below traditional cooling/heating set point with improved thermal comfort of occupants. It has a phase change material (PCM)-embedded condenser to store the rejected heat from the vapor compression cycle. Once the PCM storage is full, RoCo switches into a thermosiphon mode to re-solidify the PCM material. To obtain a better understanding of the RoCo operation and design better components, a dynamic system model capable of depicting the time-dependent performance of RoCo is developed using the Modelica language. A previously developed in-house HVAC component library, along with a newly developed PCM embedded HX model and thermosiphon model, is used to simulate both the vapor compression mode and thermosiphon mode. The simulated results are validated against the experimental data obtained from prototype tests and the model is used to optimize the cyclic operation of the device for continuous operation.

Selection and/or peer-review under responsibility of the organizers of the 12th IEA Heat Pump Conference 2017.

Keywords: Personal Cooling Device; Heat Pump; Phase Change Material; Thermosiphon; Thermosyphon; Modelica.

1. Introduction

We live in the times when global warming effects are visible and are possibly the last generation that can actually do something about it. The exponential increase in energy consumption has been the cause for the climatic changes. Heating and cooling of buildings takes up a significant 13% of primary energy in US, one of the largest energy end-users [1]. The building industry is facing two major challenges – an increased concern for the surging energy consumptions and a growing need for comfort improvements [2]. The traditional HVAC (Heating, Ventilation and Air Conditioning) systems consume large amounts of energy to maintain a uniform temperature in the ambient space within a narrow range, neither of which is really necessary for providing occupant comfort [3]. Personal cooling systems (PCS) provide an opportunity to save HVAC energy in buildings by relaxing the building thermostat settings without compromising occupant thermal comfort. By relaxing thermostat setting in either hot or cold direction, total HVAC energy is reduced at a rate of 10% per degree Celsius as reported in [4].

PCS is not a new technology and hence lots of intelligent designs have been developed which can be classified broadly as: (i) Head/Face/Upper body jets, (ii) Overhead (ceiling) fans, (iii) Side large area air flows, (iv) Chairs, heated or cooled; or ventilated and (v) Footwarmers, legwarmers, kneehole radiant panels [5]. An individual approach to the building occupants makes it possible to satisfy different needs of different people even in the ambient temperature of up to 30°C and relative humidity of up to 70% [2]. However, due to a combination of factors like poor thermal performance, bulkiness, limited mobility, high cost and poor consumer appeal, most of these devices (except for desk and ceiling fans) are not commercially available. The current ventilation standards and guidelines have very modest requirement and so the accepted level of indoor air quality may still be perceived as unacceptable to the most sensitive group (usually 20%) while the remaining people find it barely acceptable. [6]. We developed a PCS called Roving Comforter (RoCo) that addresses the issues faced by the earlier systems through its unique design.

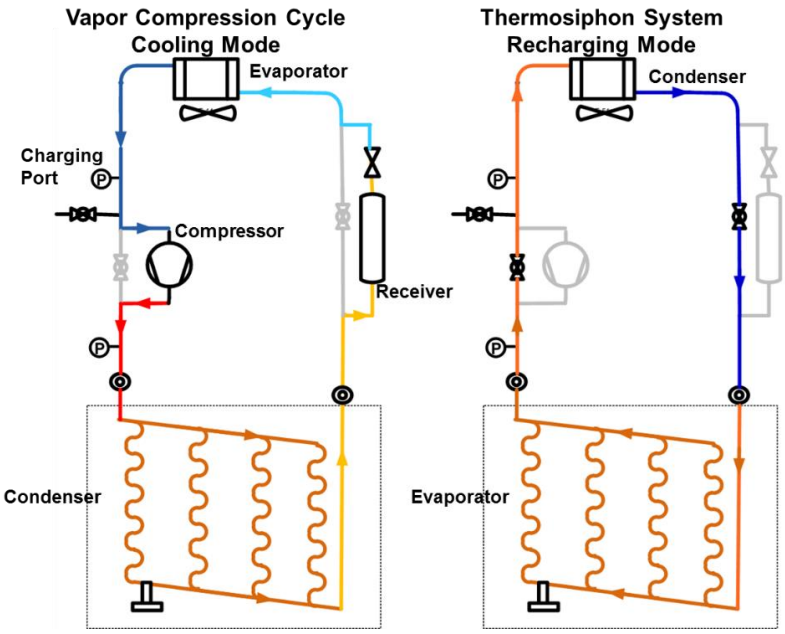

Figure 1: Schematic of the two operation modes of RoCo

2. System Description

RoCo delivers cooling using an onboard vapor compression system (VCS). The benefits of using VCS and its cost and performance comparison with other potential cooling methods were demonstrated in [7]. Figure 1 shows the schematic of the two operating modes of RoCo. The left schematic in Figure 1 shows the onboard VCS using R134a as refrigerant. The heat released by the condenser is captured by the surrounding phase change material (PCM). Thus RoCo does not release heat into the conditioned space thereby preventing addition to building heat loads. The cooling operation is terminated when the PCM surrounding the condenser is completely melted. Before the next cooling operation, there is a need to solidify the PCM (PCM recharge). This is achieved by a gravity-assisted thermosiphon operation which does not require compressor work and increase overall cycle COP. The right schematic in Figure 1 shows RoCo operating in the thermosiphon mode. Components like the compressor and the expansion valve are bypassed by turning a pair of ball valves since these components only allow refrigerant to flow in one direction and do not allow gravity assisted flow. A receiver is included in the circuit to ensure that the PCM based heat exchanger (PCM-HX) is always completely filled with liquid refrigerant at the start of thermosiphon operation and thus prevent dryout. The refrigerant circuitry is tilted in such a way to facilitate the vapor flow formed by boiling inside the PCM HX to the top of the air to refrigerant heat exchanger (AR-HX). The vapor reaches the AR-HX through the left side vertical refrigerant tube (this portion is called riser) and condenses. The fan, which blows air onto a person through the nozzle during the cooling operation, is kept on even during the

thermosiphon operation to accelerate the process. The condensed refrigerant then trickles down the right vertical refrigerant tube (this portion is called downcomer) to reach the PCM-HX and continues the cycle.

3. Modeling of Cooling Mode

As can be observed from the previous section, RoCo is fairly complex and hence a comprehensive mathematical model is essential for better understanding and design of such a system. Modelica is chosen as the platform for the modeling due to its ability to handle complex multi-domain system simulations with support for important concepts like acausal modeling and object oriented modeling. The modeling is carried out by using the updated components from CEEEModelicaLibrary (CML) [8] with the support for stream connectors [9] due to the reversing nature of flows in the system. The formulation of new components needed for the system simulation is discussed in the following subsections.

3.1. PCM-HX Component Development

The PCM-HX is modeled using an assortment of lumped control volumes (CV). The behavior of PCM is captured using two CVs: PCM Capacitor and PCM Conductor consistent with the standard approach of separating energy and momentum equation components. These control volumes are analogous to the "HeatCapacitor" and "ThermalConductor" blocks from the Thermal – HeatTransfer package of Modelica Standard Library. This approach enables development of multiple models for energy capture and heat transfer. A detailed list of the various models developed can be seen in [11] and from [12] it can be concluded that the lumped control volume approach can predict transient behavior of detailed systems to reasonable accuracy. Out of the methods presented, temperature transforming model [13] is chosen for modeling to avoid temperature oscillations of enthalpy methods and severe non-linearity of the governing equations of temperature-based equivalent heat capacity methods. The mass conservation and energy conservation equations are modeled in the PCM Capacitor block. From the results of previous work [7], it can be concluded that the natural convection during the PCM melting/solidification process cannot be neglected. However, it is very challenging to model the natural convection process without knowing the flow pattern. As a result, an empirical heat transfer coefficient as a function of the melt fraction of PCM equation is used in PCM Conductor block to avoid the detailed calculations involved in modeling PCM melting with natural convection. The correlation is based on the results of [14] and captures the effects of various flow regimes experienced during the melting.

The following assumptions are adopted to simplify the PCM capacitor formulation:

- PCM is modeled as a lumped CV to avoid modeling the momentum equations for flow of molten PCM; the variable effects of conduction and natural convection during the phase change for helical coil geometry are incorporated via the heat transfer coefficient vs melt fraction profile
- The PCM is pure and homogenous (constant thermophysical properties are applied)
- The density difference between the solid and liquid phase is less than 10% (840 kg/m^3 for liquid and 920 kg/m^3 for solid) and therefore neglected; the value of average density of these two is used
- The refrigerant tube effects on transient performance are negligible

The equation set for the PCM Conductor block is as below:

$$T^* = T_{pcm} - T_m \tag{1}$$

$$h = c(T^* + s) \tag{2}$$

The specific heat capacity c and source term s are calculated as:

$$c = \begin{cases} c_s & T^* < -\Delta T \\ \dfrac{c_s + c_l}{2} + \dfrac{h_{sl}}{2\Delta T} & -\Delta T \le T^* \le \Delta T \\ c_l & T^* > \Delta T \end{cases} \tag{3}$$

$$s = \begin{cases} \Delta T & T^* \le -\Delta T \\ \frac{c_s}{c_l}\Delta T + \frac{h_{sl}}{c_l} & T^* > -\Delta T \end{cases} \quad (4)$$

The energy equation applied to the control volume reduces to:

$$m_{pcm}\frac{dh}{dt} = \dot{Q} \quad (5)$$

The melt fraction of the control volume is determined by:

$$\lambda = \max(0, \min(1, \frac{h}{(c_s + c_l)\Delta T + h_{sl}})) \quad (6)$$

The specific enthalpy value is zero at the point when the PCM just starts to melt. For implementation in Modelica, a HeatPort element is used to calculate heat flow Q for the PkCM Capacitor block. This heat flow calculation is carried out in the PCM Conductor block which needs the melt fraction value from the PCM Conductor block.

The PCM Capacitor block takes the average value of thermal conductance, G_{avg}, as its input. It includes a first derivative continuous monotonic function thermal conductance as a function of melt fraction. The connections to both lumped refrigerant CV and Thermal Conductor block are via HeatPorts.

$$\dot{Q} = G(T_{pcm} - T_t) \quad (7)$$

The PCM-HX comprises of four parallel branches of refrigerant tubing inside the PCM. Due to flow symmetry and for the purposes of reducing the number of variables, only one branch is modeled and its result multiplied by four to obtain the performance of the whole PCM-HX. The refrigerant flow is split into four equal parts using “Flow Splitter” block and merged using “Flow Mixer” block. Finally, lumped control volumes are added before the flow splitter block ankd after the flow mixer block to model the behavior of headers at the inlet and outlet of PCM HX. The complete PCM-HX model can be seen in Figure 2.

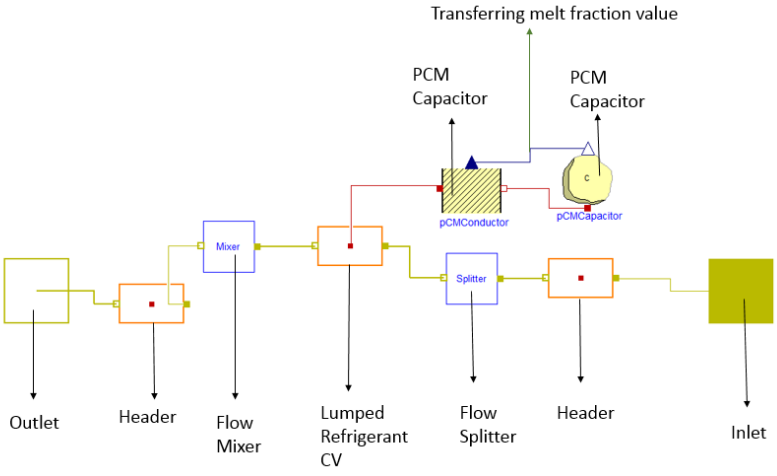

Figure 2: Modelica Block Diagram of PCM-HX

3.2. System simulation parameters

The remaining components required for the simulation are available in the CML. Brief description of input parameters for various parameters is discussed in this section. The block diagram of system simulation for the

cooling mode is shown in Figure 3. The receiver is modeled as a discrete parameter block since it contains more than 50% of the total system charge and the use of a lumped model is not sufficient to capture the refrigerant charge dynamics. To reduce the model complexity, CML uses the same approach as [15] for the pressure drop calculation of the resistance models in the library with the help of Modelica.Fluid.Utilities.regPow function by taking input values of mass flow rate and pressure drops for a steady state flow in the component for its normalized values. For heat transfer calculation, the model takes in values of single phase and average value for two phase refrigerant side heat transfer coefficient and uses a splice function to generate a smooth function for the entire range of refrigerant states. The input values for the normalized pressure drop values and heat transfer coefficients of various refrigerant states are calculated using various correlations. For pressure drop calculations, calculations are carried out using Homogeneous [16], Friedel [17], Lockhart-Martinelli [18] and Muller Steinhagen [19] correlations and a nominal value in the middle of the range of values is used. For single phase heat transfer coefficients, Dittus-Boelter correlation [20] is used. For two phase heat transfer coefficient in evaporator, chart correlation for boiling from Shah [21] is used. The condenser consists of helical coils inside heat exchanger. Calculations for helical coil parameters are carried out to find single phase liquid only heat transfer coefficient using the Schmidt correlation [22]. The single phase liquid only heat transfer coefficient is used in the latest Shah correlation [23] to obtain two phase heat transfer coefficient. Finally, the gravitational pressure drops for various components are calculated using appropriate single phase or two phase density in equation 8. For the heat exchangers, the refrigerant flow passage is discretized and the gravitational pressure drop is calculated by summation for all the volumes.

$$\Delta P_g = \rho g (H_o - H_i) \tag{8}$$

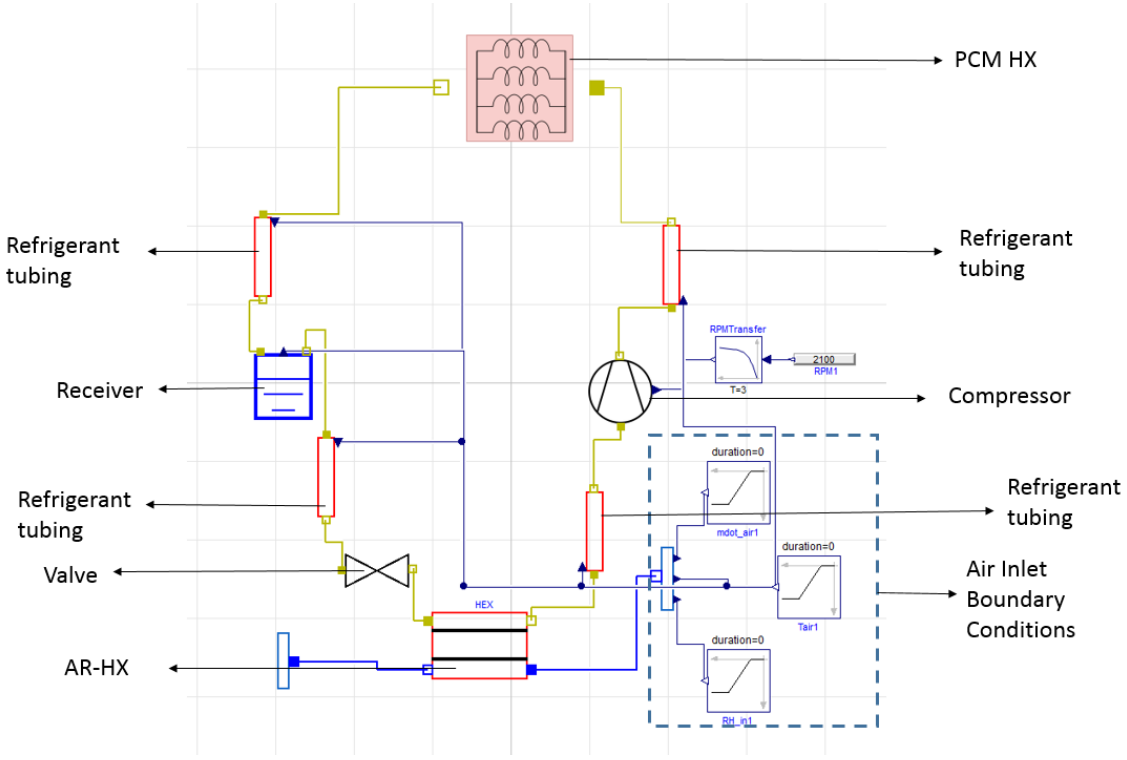

Figure 3: System model for cooling mode

4. Modeling of Recharge Mode

The cooling mode is terminated when the PCM surrounding the condenser in the cooling mode is completely melted and can be considered to be saturated with heat. It thus needs to reject the heat before its next operation. By operating a pair of ball valves, the refrigerant circuitry is modified to permit the operation of a two phase closed

thermosiphon. Its main advantage is that no mechanical pump/compressor is needed, which leads to a longer operation for a battery powered device. A detailed description of its operating mechanism and benefits can be found in the review article [24]. As pointed out by [25], it is very critical to model accurate contributions of frictional and gravitational pressure drops for modeling correct behavior. The mass flow meter installed in the circuit is bypassed during the thermosiphon operation to reduce the flow resistance in the circuit and hence there is no way to measure the mass flow rates involved during thermosiphon operation. Hence by using experimental values for air inlet and outlet temperatures alongside its volume flow rate an approximate steady state operational mass flow rate in calculated as explained in [26]. In addition, by observing the sight glass installed in circuit, it is observed that the exit of the PCM HX is vapor. For the purposes of modeling, the outlet of the PCM HX is assumed to be always a saturated vapor. This is a very reasonable assumption because after the liquid levels balance (which occurs almost instantaneously), the mass flow rate of the thermosiphon depends on the rate of evaporation from the PCM HX. The large amount of refrigerant in the receiver ensures that the downcomer is always completely filled with liquid refrigerant removing the effects of variable gravitational heads from height of the liquid column as discussed in [27]. The assumption also enables modeling without development of complicated mass flow rate correlations dependent on frictional pressure drop models as well as the void fraction models for gravitational pressure drop. The models for downcomer and riser from a previous work [26] are used alongside the new control volume developed using equations similar to the drum boiler problem of [28]. The present work improves upon [26] by including the effects of natural convection in PCM phase change and the proposed control volume, leading to a much better validation with the experimental data.

The control volume for the refrigerant inside the PCM HX in the thermosiphon mode is shown in Figure 4. The refrigerant tubes are vertical with liquid refrigerant entering from the bottom. After the liquid levels have balanced, the mass flow rate exiting the outlet is vapor. The control volume has an inlet and outlet modeled using FluidPorts (Modelica.Fluid.Interfaces.FluidPort), while the heat transfer is using the HeatPort connector (Modelica.Thermal.HeatTransfer.Interfaces.HeatPort_a). Since the control volume is lumped, the black dot at the center of figure 4, represents the location of the fluid element.

The total volume of the refrigerant tube consists of the volume occupied by the vapor and the volume occupied by the liquid refrigerant. Out of the two properties required to determine the refrigerant state, first (the average density) can be calculated as follows:

$$V_{tot} = V_l + V_s \tag{9}$$

$$m = \rho_l V_l + \rho_v V_v \tag{10}$$

$$\rho_{avg} = \frac{m}{V_{tot}} \tag{11}$$

The second property (pressure), can be obtained by averaging the pressure at the inlet and outlet.

$$P_{avg} = \frac{P_i + P_o}{2} \tag{12}$$

These two properties are sufficient to determine the state of refrigerant, and all the remaining properties are calculated. The heat transfer coefficient for heat transfer from the heat port is given as an input. Since enthalpy in the FluidPort is defined as a stream variable [9], only outlet enthalpies need to be set for the inlet and outlet. The outlet enthalpy at the outlet is set as saturated vapour enthalpy while the outlet enthalpy at the inlet port is set as saturated liquid enthalpy. The mass conservation and energy conservation equations are used to update pressure and specific enthalpy which are the state variables.

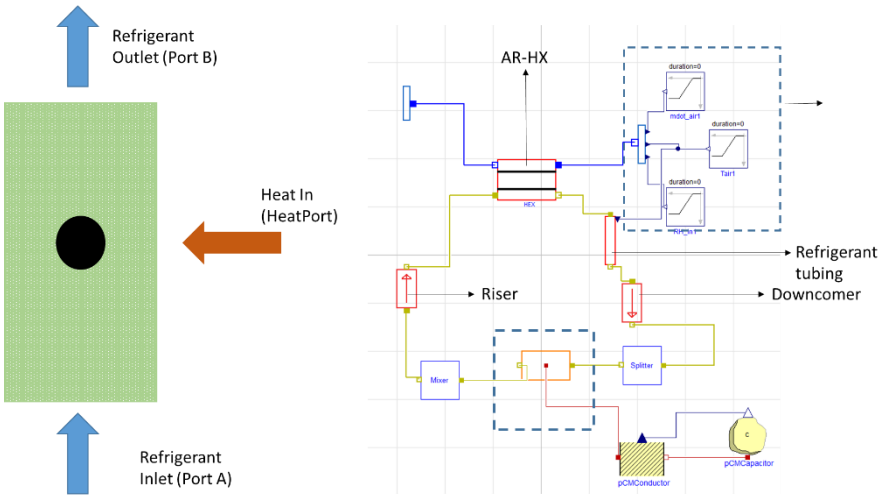

Figure 4: System model of thermosiphon with the schematic for boxed CV on left

5. Results and Discussion

Figures 5 and 6 show the results of cooling mode plotted against the experimental results. As can be observed from figure 5, the model is able to predict the overall transients of the cooling mode to a reasonable extent. In the initial period of roughly 20 minutes when the PCM heat capture is sensible, the discharge pressure in simulation rises much faster and then progresses slower than the experimental case. The difference can be attributed to the inaccuracy of heat transfer coefficient correlation of the PCM as well as the valve model which operates with the assumption of constant discharge coefficient. In the experimental setup, a variable expansion valve is used and constantly modulated to maintain a constant superheat temperature. However, the model accurately predicts the time period when the melting starts. Figure 6 shows the cooling capacity as well as the power consumption of compressor. The setup uses a very small 1.4 cc compressor and the experimental data is not available for the

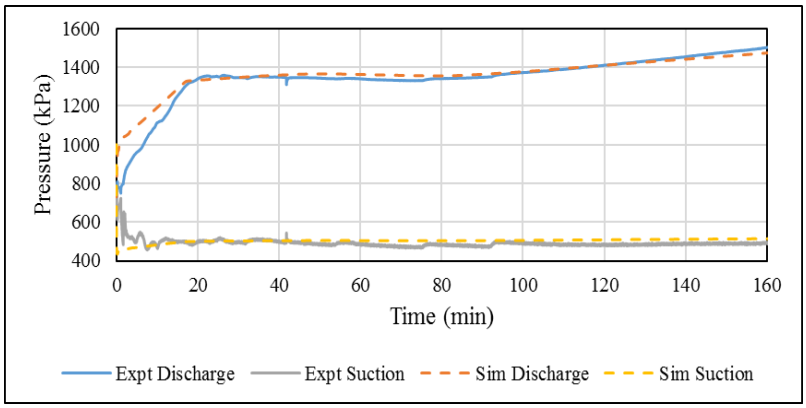

Figure 5: Pressure range of operation in the cooling mode

operation conditions. The values of inefficiencies are adjusted to match the experimental results. The model slightly under predicts the cooling capacity. This can be attributed to a combination of factors like uncertainty of experimental results, uncertainty in heat transfer prediction from the correlations and also to mismatch in

prediction of heat losses in various portions of refrigerant tubing which is not measured and hence cannot be compared to the heat losses in simulation.

Figure 6: Cooling capacity and the compressor power

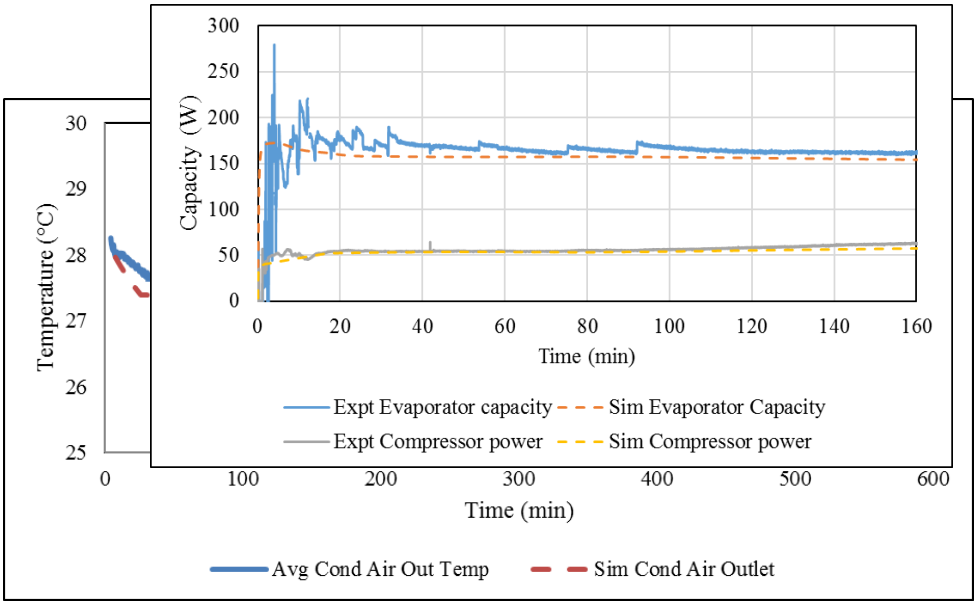

Figure 7: Air outlet temperature from AR-HX during thermosiphon

During the operation of thermosiphon, the mass flow meter is bypassed to reduce the pressure drops in the circuit. As a result, the mass flow rate in the circuit is not measured and hence for comparison the air outlet temperature of the AR-HX is plotted in figure 7. The deviations can be attributed to the assumption of constant specific heat capacity in the melting range arising from temperature transforming model. However, it is observed from the DSC data that this assumption is not correct. For the purpose of simulation, however the glide range and melting point are hence adjusted to obtain the same solidification period as the experiment. However, the temperature at the end of solidification in the experiment and the simulation do not match and this results in the difference. This behaviour of PCM does not affect the VCC simulation because the mass flow rate is due to the compressor, while in thermosiphon it is due to the boiling of refrigerant in the PCM HX and hence the temperature of the heat source becomes critical. The maximum deviation due to this error in outlet air temperature prediction is 1°C.

Finally, the variation of melt fraction in a continuous cooling and recharge operation is plotted against time as seen in Figure 8. The plot shows 5 regions which are identified as: (1) Sensible heating of solid PCM, (2) Melting,

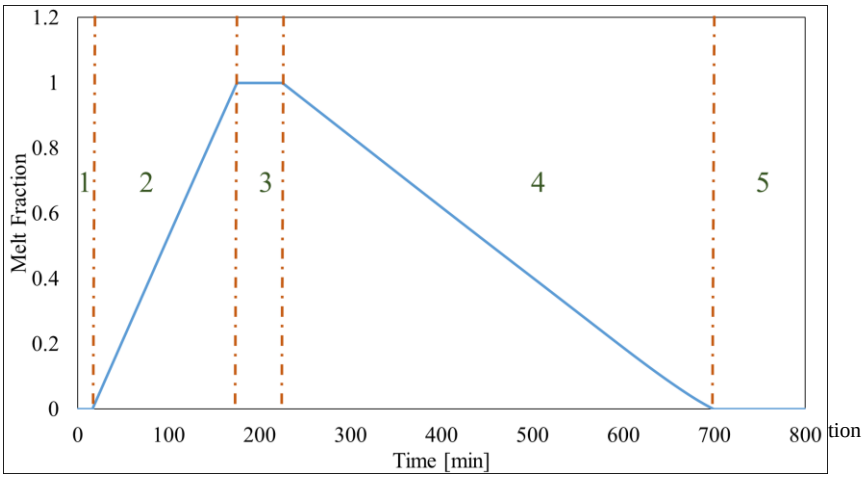

(3) Region of switching over to thermosiphon, (4) Solidification and (5) Sensible cooling PCM. The device is intended to store heat in the form of latent energy and so it is desirable to alternate between regions 2 and 4 without going into regions 1, 2 and 3 during the continuous operation. The time period of region 2 is 158 minutes and for region 4 is 474 minutes. Total runtime of both operations in tandem will take 632 minutes. Thus it is possible to have two cooling operations of slightly more than 5 hours with the current device.

6. Conclusions

An innovative portable personal cooling device called RoCo is being developed to provide better thermal comfort to occupants with energy savings in the range of 10-30%. It uses vapor compression cycle to provide cooling and stores heat into a PCM storage which is recharged by a gravity assisted thermosiphon operation. Dynamic modeling is carried out to optimize the timings of both the processes using Modelica. Temperature transforming model is used for modeling the PCM behavior. The operation time for the cooling operation is 158 minutes while that for recharge is 474 minutes.

Nomenclature

c	[J/kg-K]	Specific heat capacity
g	[m/s^2]	Acceleration due to gravity
G	[W/K]	Thermal conductance
h	[J/kg]	Specific enthalpy
H	[m]	Height
λ	[-]	Melt fraction
m	[kg]	Mass
P	[Pa]	Pressure
$\dot{Q}$	[W]	Rate of heat transfer
ρ	[kg/m^3]	Density
s	[K]	Source term in temperature transforming model
t	[s]	time
ΔT	[K]	Half width of the temperature glide range
T	[K]	Temperature
T*	[K]	Scaled Temperature
V	[m^3]	Volume

Subscripts

avg	Average
g	Gravity
i	Inlet
l	Liquid phase
m	Mid-point of melting temperature glide
o	Outlet
pcm	Lumped phase change material control volume
s	Solid phase
sl	Solid to liquid phase change
t	Refrigerant tube
tot	Total

Acknowledgements

The authors are grateful to the Advanced Research Projects Agency - Energy (ARPA-E) for funding the project with Award Number DE-AR0000530. The contributions of the Center for Environmental Energy Engineering at University of Maryland is also acknowledged.

References

[1] Buildings Technologies Program, Energy Efficiency and Renewable Energy, *U.S. Department of Energy: 2011 Buildings Energy Data Book*, March 2012
[2] Vesely M, Zeiler Wim. (2014). Personalized conditioning and its impact on thermal comfort and energy performance – A review. *Renewable and Sustainable Energy Reviews* 2014;**34**:401-408.
[3] Hoyt T, Kwang HL, Zhang H, Arens E, Webster T. (2009). Energy Savings from Extended Air Temperature Setpoints and Reductions in Room Air Mixing, *International conference on Environmental Ergonomics, Boston*, August 2–7; 2009.
[4] Hoyt, Tyler; Arens, Edward; & Zhang, Hui. (2014). Extending air temperature setpoints: Simulated energy savings and design considerations for new and retrofit buildings. *Building and Environment*. doi: 10.1016/j.buildenv.2014.09.010.
[5] Zhang, Hui; Arens, Edward; & Zhai, Yongchao. (2015). A review of the corrective power of personal comfort systems in non-neutral ambient environments. *Building and Environment*, **91**, 15 - 41. doi: 10.1016/j.buildenv.2015.03.013.
[6] Ole Fanger, P. (2006), What is IAQ?. Indoor Air, 16: 328–334. doi:10.1111/j.1600-0668.2006.00437
[7] Dhumane, R., Ling, J. et al. (2016). Transient Multiphysics Modeling of a Robotic Personal Air-Conditioning Device. *Proceedings of 16th International Refrigeration and Air Conditioning Conference, Purdue, Indiana, USA*.
[8] Qiao,H., Aute, V., Radermacher, R. (2014). Transient modeling of a flash tank vapor injection heat pump system – Part I: Model development. *International Journal of Refrigeration*; **49**: 169-182 doi:10.1016/j.ijrefrig.2014.06.019
[9] Franke, R., Casella, F., et. al (2009). Stream Connectors – An extension of Modelica for Device Oriented Modeling of Convective Transport Phenomena. *Proceedings of 7th Modelica Conference*, Como, Italy, Sep. 20-22, 2009.
[10] Wang, S., Faghri, A., Bergman, T. (2010). A comprehensive numerical model for melting with natural convection. *International Journal of Heat and Mass Transfer*; **53**: 1986-2000 doi:10.1016/j.ijheatmasstransfer.2009.12.057
[11] Hu, H., Argyropoulos, A. (1996). *Mathematical modelling of solidification and melting: a review*. *Modelling and Simulation in Materials Science and Engineering*; **4**: 371-396
[12] Leonhardt, C., Muller, D. (2009). Modelling of Residential Heating Systems using a Phase Change Material Storage System. Proceedings of 7th Modelica Conference, Como, Italy, Sep. 20 – 22, 2009.
[13] Cao, Y., Faghri, A. (1990). A numerical analysis of phase change problem including natural convection. *ASME Journal of Heat Transfer*; **112**: 812-815
[14] Sparrow EM, Patankar SV, Ramadhyani SS. (1977). Analysis of Melting in the Presence of Natural Convection in the Melt Region. *ASME Journal of Heat Transfer*; **99**(4):520-526. doi:10.1115/1.3450736.
[15] Wetter, M. (2009). Modelica Library for Building Heating, Ventilation and Air Conditioning Systems. *Proceedings of 7th Modelica Conference*, Italy, Sep. 20-22, 2009.
[16] Adams, M., Woods, W., Bryan, R. (1942) Vaporization inside horizontaltubes-ii-benzeno–oil mixtures, *ASME Transactions* **64**
[17] Friedel, L. (1979). Improved friction pressure drop correlations for horizontal andvertical two-phase pipe flow, *European Two-Phase Flow Group Meeting*, Ispra, Italy, Paper E2
[18] Lockhart, R., Martinelli, R. (1949). Proposed correlation of data for isothermal two-phase, two-component flow in pipes, *Chemical Engineering Progress* **45**; 39–48
[19] Muller-Steinhagen, H., Heck, K. (1986) A simple friction pressure drop correlation for two-phase flow pipe, Chemical Engineering Process. **20**: 297–308
[20] Dittus, F., Boelter, L. (1985) Heat Transfer in Automobile Radiators of the Tubular Type, International Communications in Heat and Mass Transfer 12 (1) 3-22.
[21] M.M. Shah, (1982) Chart Correlation for Saturated Boiling Heat Transfer: Equations and Further Study, *ASHRAE Transactions* **88** (1): 185-196.
[22] Schmidt, E. (1967) Warmeubergang und Druckverlust in Rohrschlangen.*Chem -Ing -Techn* **39**:781–789
[23] Shah, M. (2016). Comprehensive correlations for heat transfer during condensation in conventional and min/micro channels in all orientations. *International Journal of Refrigeration*. **67**: 22-41
[24] Jadhav, A., Patil, S. (2016). Two phase thermosyphon – A review of studies. *International journal of engineering sciences and Research Technology*; **5**(1): 193-205
[25] Khodabandeh,R. (2005). Pressure drop in riser and evaporator in an advanced two-phase thermosyphon loop. International Journal of Refrigeration; **28**(5): 725-734

[26] Dhumane, R., Mallow, A., et. al. (2016). Transient Modeling of a Thermosiphon based Air Conditioner with Compact Thermal Storage: Modeling and Validation
[27] Zhang, P., Wang, B., et. al. (2015). Modeling and performance analysis of a two phase thermosyphon loop with partially/fully liquid-filled downcomer. International Journal of Refrigeration; **58**: 172-185
[28] Franke, R., Kruger, K. (2003). On-line Optimization of Drum Boiler Startup. *Proceedings of the 3rd International Modelica Conference*, Linkoping, Sweden, Nov 3-4, 2003.